Influenza A virus superinfection potential is regulated by viral genomic heterogeneity

Jiayi Sun[1] and Christopher B. Brooke[1,2*]

[1]Department of Microbiology; University of Illinois, Urbana, IL 61801
[2]Carl R. Woese Institute for Genomic Biology; University of Illinois, Urbana, IL 61801
[*]Corresponding author (cbrooke@illinois.edu)

Abstract

Defining the specific factors that govern the evolution and transmission of influenza A virus (IAV) populations is of critical importance for designing more effective prediction and control strategies. Superinfection, the sequential infection of a single cell by two or more virions, plays an important role in determining the replicative and evolutionary potential of IAV populations. The prevalence of superinfection during natural infection, and the specific mechanisms that regulate it, remain poorly understood. Here, we used a novel single virion infection approach to directly assess the effects of individual IAV genes on superinfection efficiency. Rather than implicating a specific viral gene, this approach revealed that superinfection susceptibility is determined by the total number of viral genes expressed, independent of their identity. IAV particles that expressed a complete set of viral genes potently inhibit superinfection, while semi-infectious particles (SIPs) that express incomplete subsets of viral genes do not. As a result, virus populations that contain more SIPs undergo more frequent superinfection. These findings identify both a major determinant of IAV superinfection potential and a prominent role for SIPs in promoting viral co-infection.

Introduction

Influenza A viruses (IAV) are estimated to cause hundreds of thousands of deaths across the world every year during seasonal epidemics, despite widespread pre-exposure and vaccination(1). In addition to the yearly burden of seasonal influenza viruses, novel zoonotic IAV strains periodically emerge into humans from swine or birds, triggering unpredictable pandemics that can dramatically increase infection and mortality rates (2). Defining the specific factors that influence the evolution of influenza viruses is critical for designing more effective vaccines, therapeutics, and surveillance strategies.

The prevalence of co-infection can play an enormous role in determining the replicative and evolutionary potential of IAV populations. This is a function both of the segmented nature of the viral genome and the enormous amount of genomic heterogeneity present within IAV populations(3,4). Co-infection allows reassortment, the production of novel viral genotypes through the intermixing of the individual IAV genome segments (5,6). Reassortment events have contributed to the emergence of every major influenza pandemic of the past century(7). Co-infection also facilitates the complementation and productive replication of the semi-infectious particles (SIPs) that make up the majority of

1

46 IAV populations (8–12). Finally, increasing the frequency of co-infection can accelerate
47 viral replication kinetics and virus output by increasing the average multiplicity of infection
48 (MOI)(13–15). Thus to better understand how IAV populations transmit and evolve, we
49 must identify the specific host and viral factors that govern co-infection.
50
51 One of the primary means by which co-infection can occur is superinfection, the
52 sequential infection of one cell by multiple viral particles. For some viruses, superinfection
53 appears to occur freely(16,17). In contrast, a diverse range of viruses actively inhibit
54 superinfection through a variety of mechanisms, a phenomenon known as superinfection
55 exclusion (SIE)(18–26). The only in-depth study to date of IAV superinfection concluded
56 that the viral neuraminidase (NA) protein acts to potently and rapidly inhibit IAV
57 superinfection by depleting infected cells of the sialic acid receptors required for viral entry
58 (27). More recently, Dou et al. reported a narrow time window during which IAV
59 superinfection was possible(13). The existence of a potent mechanism of IAV SIE is at
60 odds with both the frequent co-infection observed in a variety of experimental settings,
61 and the widespread occurrence of reassortment at the global scale(28–33). Marshall et
62 al. showed that superinfection up to 8 hours after primary infection leads to robust co-
63 infection and reassortment in cell culture(34). Widespread co-infection and
64 complementation have also been observed in the respiratory tracts of IAV-infected mice
65 and guinea pigs(9,35). Collectively, these results suggest that IAV superinfection can be
66 restricted, but to what extent and through which specific mechanisms remains a crucial
67 open question.
68
69 Here, we reveal that IAV superinfection potential is directly regulated by the extent of
70 genomic heterogeneity within the viral population. We observed that superinfection
71 susceptibility is determined in a dose-dependent fashion by the number of viral genes
72 expressed by the initially infecting virion, regardless of their specific identity. Further, we
73 show that superinfection occurs more frequently in IAV populations with more SIPs
74 compared with those with fewer. Finally, we demonstrate that SIE is mediated by the
75 presence of active viral replication complexes, and is completely independent of gene
76 coding sequence. Altogether, our results reveal how genomic heterogeneity influences
77 IAV superinfection potential, and demonstrate how SIPs can modulate collective
78 interactions within viral populations.
79
80 **Results**
81
82 **Influenza virus SIE occurs in multiple cell types and is independent of type I**
83 **interferon secretion**
84 A previous study of IAV SIE concluded that NA expression completely blocks
85 susceptibility to superinfection by 6 hours post-infection (hpi)(27). To explore the potential
86 mechanisms of IAV SIE in greater detail, we developed a flow cytometry-based assay
87 that allows us to precisely measure the effects of previous infection on superinfection
88 efficiency. To clearly identify cells infected by the first virus, the superinfecting virus, or
89 both, we used two recombinant viruses that express antigenically distinct hemagglutinin
90 (HA), NA, and NS1 proteins that we could distinguish using specific monoclonal
91 antibodies (mAbs) that we had on hand (**Fig S1**). For the primary infection, we used a

2

92 recombinant version of the H1N1 strain A/Puerto Rico/8/34 (rPR8). For the secondary
93 infection, we used a recombinant virus (rH3N2) that contained the HA and NA gene
94 segments from the H3N2 strain A/Udorn/72, the NS gene segment from
95 A/California/04/09, and the remaining 5 segments from PR8.
96
97 We first asked whether prior infection with rPR8 affected cellular susceptibility to
98 superinfection with rH3N2. We infected MDCK cells with rPR8 at an MOI of <0.3
99 TCID50/cell, and at 3 hpi (all times post infection will be relative to the first virus added)
100 we added the PR8-HA-specific neutralizing mAb H17-L2 to block secondary spread of
101 rPR8 within the culture. At 6 hpi, we infected with rH3N2 at an MOI of <0.3 TCID50/cell.
102 To prevent spread of both rPR8 and rH3N2, we added 20 mM NH4Cl at 9 hpi. In parallel,
103 we performed simultaneous co-infections (0 hr) with rPR8 and rH3N2 to measure co-
104 infection frequencies when SIE should not be possible. At 19 hpi we harvested cells and
105 examined primary and secondary virus infection by flow cytometry, using H1 and H3
106 expression as markers of rPR8 and rH3N2 infection, respectively. We observed that the
107 H3+ frequency within H1+ cells was significantly reduced when rPR8 infection preceded
108 rH3N2 by 6 hrs compared with when rPR8 and rH3N2 were added simultaneously (**Fig
109 1A**). This indicated that rPR8 infection significantly reduces the susceptibility of cells to
110 superinfection by 6 hpi.
111
112 We next asked whether the SIE effect was cell type specific, and whether it depended
113 upon activation of the type I interferon (IFN) system. We performed the same experiment
114 as above in MDCK cells, A549 cells, 293T, and Vero cells (which are incapable of type I
115 IFN secretion)(36,37). We observed that the extent of SIE was comparable between all
116 cell lines tested, suggesting that SIE occurs in multiple distinct cell types, and does not
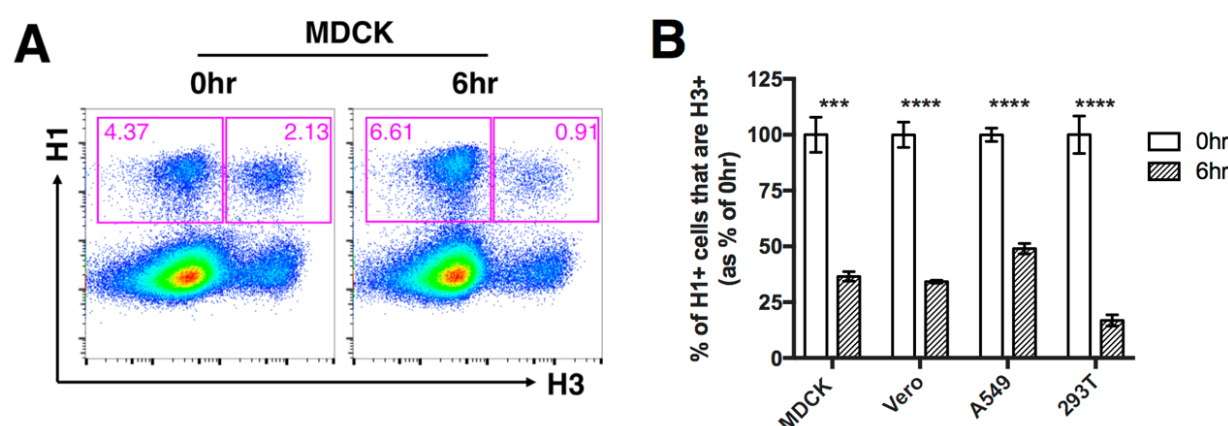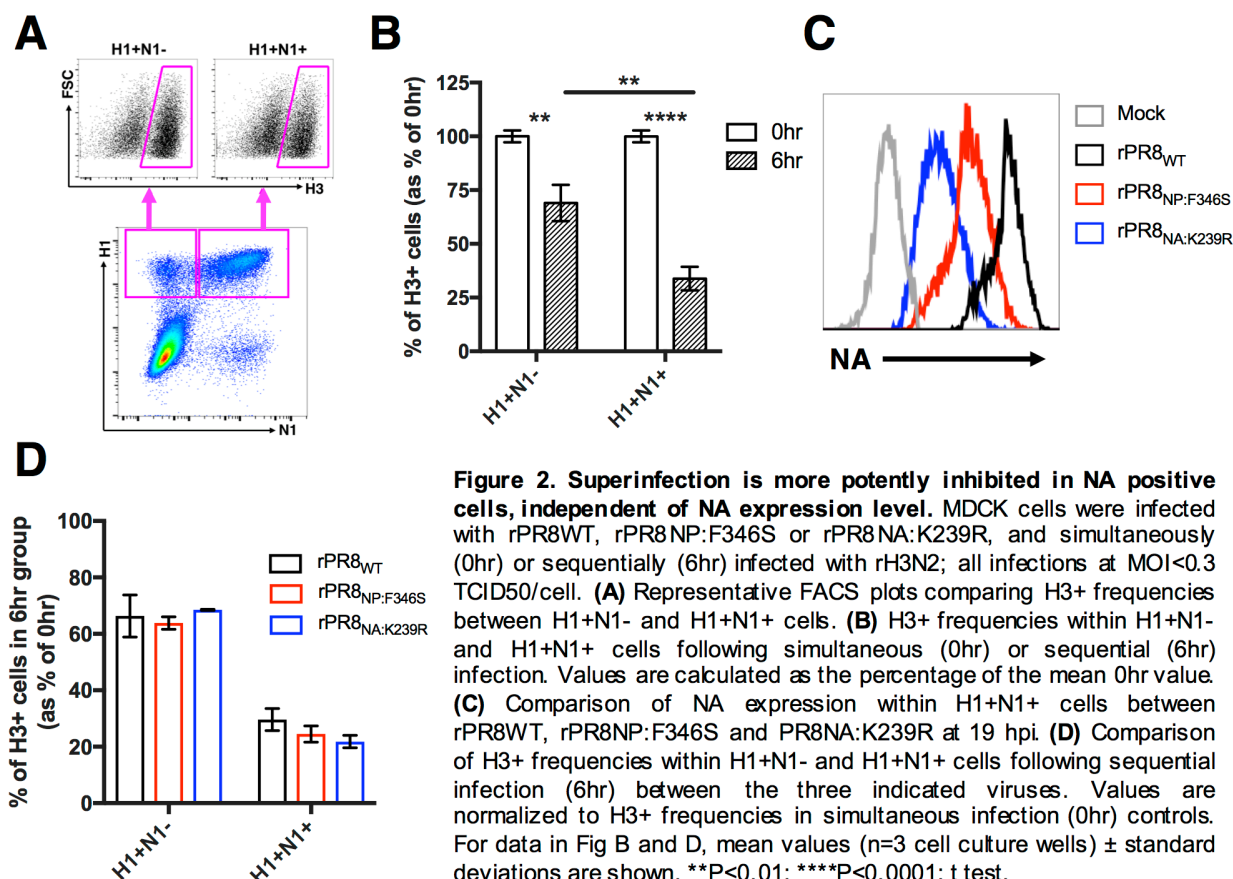117 depend upon IFN secretion (**Fig 1B; Fig S2**).
118

Figure 1. A 6-hr delay between primary infection and superinfection allows robust superinfection exclusion. The indicated mammalian cell lines were either simultaneously (0hr) or sequentially (6hr) infected with rPR8 and rH3N2 at MOI<0.3 TCID50/cell. **(A)** Representative FACS plots showing expression of H1 versus H3 within MDCK cells. **(B)** H3+ frequencies within H1+ cells following simultaneous or sequential infection, in the indicated cell lines. Values are calculated as the percentage of the mean 0hr value, and are presented as the mean (n=3 cell culture wells) ± standard deviations. ***P<0.001;****P<0.0001;t test.

119

3

Viral neuraminidase expression does not fully explain the SIE phenotype

In an attempt to confirm the previously reported role for NA activity in SIE, we directly measured the effect of NA expression on IAV SIE in our system(27). We took advantage of our previous observation that IAV populations consist primarily of SIPs that fail to express one or more viral genes(8). When carrying out the primary infection at low MOI, we generate populations of infected cells that are either positive or negative for expression of a given viral gene. We can then assess the effects of specific viral proteins on superinfection susceptibility by comparing superinfection frequencies between infected cells that do or do not express the protein in question.

We performed the same superinfection experiment as described above in MDCK cells, and at 19 hpi, harvested and stained with mAbs against H1, N1, and H3. To compare rPR8 infected cells that did or did not express NA, we individually gated cells into H1+N1+ and H1+N1- subpopulations (**Fig 2A**). Comparison of H3+ frequencies between H1+N1+ and H1+N1- cells revealed that NA expression was clearly associated with decreased susceptibility to superinfection in rPR8-infected cells (**Fig 2B**). This finding was consistent with the previously reported role for NA in IAV superinfection exclusion(27). Importantly, while SIE was most pronounced in the H1+N1+ cells, we also observed a significant decrease in superinfection susceptibility within the H1+N1- cell population by 6hpi, suggesting that viral factors other than NA also act to restrict superinfection.

Figure 2. Superinfection is more potently inhibited in NA positive cells, independent of NA expression level. MDCK cells were infected with rPR8WT, rPR8NP:F346S or rPR8NA:K239R, and simultaneously (0hr) or sequentially (6hr) infected with rH3N2; all infections at MOI<0.3 TCID50/cell. **(A)** Representative FACS plots comparing H3+ frequencies between H1+N1- and H1+N1+ cells. **(B)** H3+ frequencies within H1+N1- and H1+N1+ cells following simultaneous (0hr) or sequential (6hr) infection. Values are calculated as the percentage of the mean 0hr value. **(C)** Comparison of NA expression within H1+N1+ cells between rPR8WT, rPR8NP:F346S and PR8NA:K239R at 19 hpi. **(D)** Comparison of H3+ frequencies within H1+N1- and H1+N1+ cells following sequential infection (6hr) between the three indicated viruses. Values are normalized to H3+ frequencies in simultaneous infection (0hr) controls. For data in Fig B and D, mean values (n=3 cell culture wells) ± standard deviations are shown. **P<0.01; ****P<0.0001; t test.

142 Relative NA activity can vary significantly between IAV strains(38). If NA activity inhibits
143 IAV superinfection, we hypothesized viruses that express less NA would undergo more
144 frequent superinfection. To define the quantitative relationship between NA expression
145 and SIE, we examined the effects of two substitutions (NP:F346S and NA:K239R) that
146 decrease cellular NA expression relative to wild-type PR8 on superinfection
147 efficiency(9,39) (**Fig 2C**). Surprisingly, these mutants did not exhibit higher superinfection
148 frequencies than wild-type PR8 (**Fig 2D**). These results suggest that SIE can be mediated
149 by NA gene expression, but is not significantly influenced by relative NA expression levels.
150
151 **Superinfection susceptibility is determined by the number of viral genes expressed,**
152 **not their identity**
153 Based on our observation that superinfection was also inhibited within H1+N1- cells (**Fig**
154 **2B**), we hypothesized that expression of other viral gene products can also inhibit
155 superinfection. We examined the effects of HA and NS1 expression on superinfection
156 susceptibility, using rPR8-specific mAbs. Surprisingly, we found that both HA and NS1
157 expression within rPR8-infected cells were also associated with significant decreases in
158 superinfection by rH3N2, comparable to the effect associated with NA expression (**Fig**
159 **3A,B**). To further dissect the effects of viral gene expression patterns on SIE, we
160 individually gated all seven possible combinations of HA, NA, and NS1 expression by
161 rPR8 (HA+NA+NS1+, HA+NA+, HA+NS1+, NA+NS1+, HA+, NA+, NS1+) and directly
162 compared rH3N2 infection frequencies between them (gating scheme: **Fig. S3**). We
163 observed that the fraction of cells superinfected with rH3N2 was inversely correlated with
164 the number of rPR8 genes expressed, regardless of their specific identities (**Fig 3C,D**).
165 Thus, susceptibility to IAV superinfection is determined by the number of viral genes
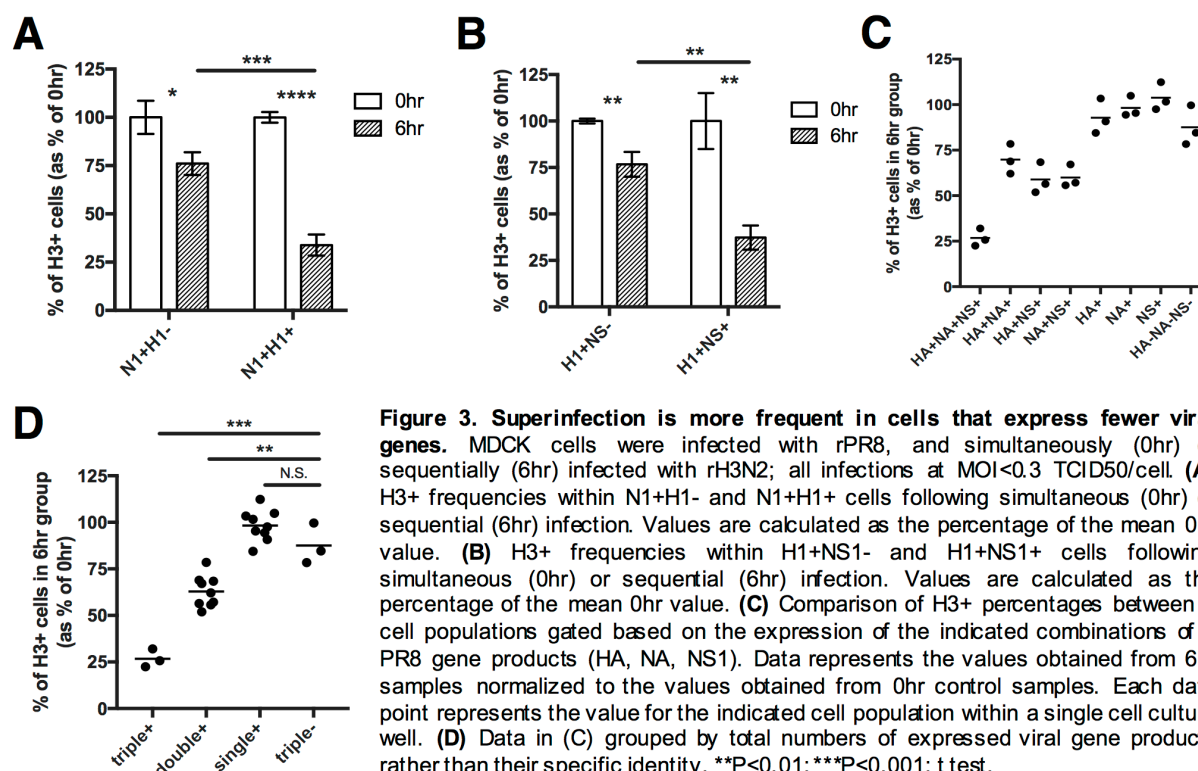166 expressed in the host cell, rather than their specific identity.

Figure 3. Superinfection is more frequent in cells that express fewer viral genes. MDCK cells were infected with rPR8, and simultaneously (0hr) or sequentially (6hr) infected with rH3N2; all infections at MOI<0.3 TCID50/cell. **(A)** H3+ frequencies within N1+H1- and N1+H1+ cells following simultaneous (0hr) or sequential (6hr) infection. Values are calculated as the percentage of the mean 0hr value. **(B)** H3+ frequencies within H1+NS1- and H1+NS1+ cells following simultaneous (0hr) or sequential (6hr) infection. Values are calculated as the percentage of the mean 0hr value. **(C)** Comparison of H3+ percentages between 8 cell populations gated based on the expression of the indicated combinations of 3 PR8 gene products (HA, NA, NS1). Data represents the values obtained from 6hr samples normalized to the values obtained from 0hr control samples. Each data point represents the value for the indicated cell population within a single cell culture well. **(D)** Data in (C) grouped by total numbers of expressed viral gene products rather than their specific identity. **P<0.01; ***P<0.001; t test.

167

5

Superinfection is more prevalent in IAV populations with more SIPs

If the number of viral genes expressed in a cell determines superinfection susceptibility, then decreasing the average number of functional viral genes successfully delivered by individual virions should increase the overall incidence of superinfection. We tested this by artificially decreasing the functional gene segment content of rPR8 through exposure to UV irradiation(40). Exposure to low dose UV irradiation generates SIPs that carry gene-lethal UV-induced lesions at frequencies proportional to genome segment length. Based on our previous findings, we hypothesized that superinfection frequencies would increase with longer exposure of rPR8 to UV.

We UV irradiated (302nm) rPR8 for either 30s or 60s, and confirmed that the TCID50 concentration was reduced and the SIP concentration was increased as a function of treatment duration (**Fig 4A-C**). We then performed superinfection assays as before, comparing rH3N2 superinfection frequencies between untreated and UV-irradiated rPR8 in MDCK cells. To fairly compare superinfection frequency between viral populations with differing particle-to-infectivity ratios, we normalized our rPR8 infections based on equivalent numbers of particles capable of expressing NA (NA-expressing units; NAEU)(9).

We first examined the effect of UV treatment on superinfection when rPR8 and rH3N2 were added to cells simultaneously (0hr). This was a critical control because UV treatment can increase the measured incidence of co-infection independent of SIE effects, purely by creating a larger pool of SIPs that only show up in our assays when complemented by secondary infection(40). Consistent with this, we observed a small increase in co-infection frequency with UV treatment when both viruses were added simultaneously (**Fig 4D,E**). When rH3N2 was added 6 hours after rPR8 however, we observed a much more pronounced increase in superinfection frequency with UV treatment, consistent with our hypothesis that superinfection is regulated by the proportion of SIPs present within the viral population (**Fig 4D-F**).

SIE is mediated by active IAV replication complexes, and is independent of gene coding sequence

Our data reveal that IAV superinfection potential is determined by the number of viral genes expressed within a cell, independent of their specific identity. This suggests that the viral gene products themselves are dispensable for SIE. We thus hypothesized that active replication and/or transcription of viral RNAs by the viral replicase complex is responsible for decreasing cellular susceptibility to subsequent infection. To test this, we co-transfected 293T cells with pDZ vectors encoding the individual viral replicase proteins (PB2, PB1, PA, and NP) together with a pHH21 vector encoding either the HA vRNA gene segment (HA$_{vRNA}$) or a vRNA-derived reporter gene segment in which the eGFP ORF is flanked by the 5' and 3' UTR sequences from the NA segment (eGFP$_{vRNA}$). These UTR sequences are required for replication and transcription of the reporter RNA by the viral replicase. 24 hours post transfection, we infected cells with rH3N2 at an MOI of 0.2 TCID50/cell and measured infectivity at 8 hpi using an M2-specific mAb.
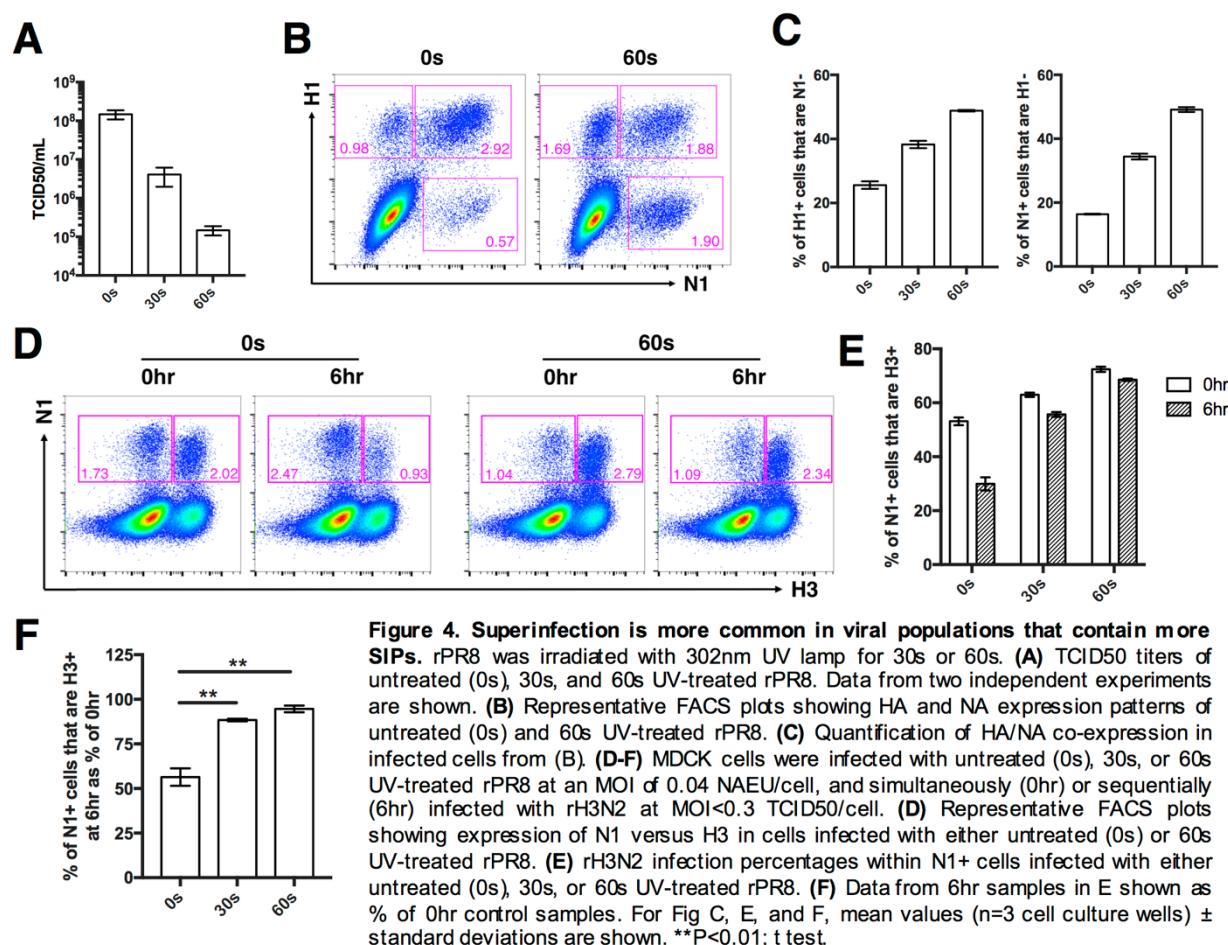
6

Figure 4. Superinfection is more common in viral populations that contain more SIPs. rPR8 was irradiated with 302nm UV lamp for 30s or 60s. **(A)** TCID50 titers of untreated (0s), 30s, and 60s UV-treated rPR8. Data from two independent experiments are shown. **(B)** Representative FACS plots showing HA and NA expression patterns of untreated (0s) and 60s UV-treated rPR8. **(C)** Quantification of HA/NA co-expression in infected cells from (B). **(D-F)** MDCK cells were infected with untreated (0s), 30s, or 60s UV-treated rPR8 at an MOI of 0.04 NAEU/cell, and simultaneously (0hr) or sequentially (6hr) infected with rH3N2 at MOI<0.3 TCID50/cell. **(D)** Representative FACS plots showing expression of N1 versus H3 in cells infected with either untreated (0s) or 60s UV-treated rPR8. **(E)** rH3N2 infection percentages within N1+ cells infected with either untreated (0s), 30s, or 60s UV-treated rPR8. **(F)** Data from 6hr samples in E shown as % of 0hr control samples. For Fig C, E, and F, mean values (n=3 cell culture wells) ± standard deviations are shown. **P<0.01; t test.

Infection frequencies were decreased ~50% in cells expressing the replicase components plus the eGFP$_{vRNA}$ construct, compared with control cells transfected with the replicase-expressing constructs plus an empty pHH21 vector (**Fig 5A**). When comparing rH3N2 infectivity between co-transfected cells (eGFP+, HA+) and un-co-transfected cells (eGFP-, HA-) within the same culture wells, the inhibitory effects mediated by eGFP$_{vRNA}$ or HA$_{vRNA}$ expression were comparable (**Fig 5B,S4**). Importantly, this effect was not seen when we left out the plasmid encoding PA (RNP$_{PA-}$) or used an eGFP reporter RNA that lacked the viral UTR sequences (eGFP$_{ORF}$) (**Fig 5A**). Altogether, these data indicate that the inhibition of infection requires both an intact replicase complex and an RNA template containing the viral UTR sequences, but not the viral coding sequence.

Our data demonstrate that IAV SIE is mediated by the specific activity of viral replication complexes. One potential explanation is that large amounts of recently-synthesized negative sense vRNA within the cell might outcompete incoming genome segments for replication and expression. To test this, we transfected 293T cells with a pHH21 vector that overexpresses the eGFP$_{vRNA}$ segment, and measured susceptibility to rH3N2 infection 24 hours later using an NP-specific mAb. Compared to the empty vector control, we observed no effect of eGFP$_{vRNA}$ vRNA overexpression on cellular susceptibility to infection (**Fig 5C**). Similarly, we observed no effect when we overexpressed the cRNA or

7

233 vRNA forms of the HA gene segment, either individually or together (**Fig 5C**). Another
234 potential explanation is that viral mRNA or protein overexpression might inhibit
235 subsequent infection. To test this, we transfected 293T cells with pCI vectors that
236 overexpress mRNA and protein of eGFP and HA, and measured susceptibility to rH3N2
237 infection 24 hours post transfection using the M2-specific mAb. Compared to empty
238 vector control, mRNA/protein overexpression of eGFP or HA had no effect on the
239 following infection (**Fig 5D, S5A, S5B**). Altogether, these data demonstrate that IAV SIE
240 is driven by the presence of active viral replication complexes, rather than the protein or
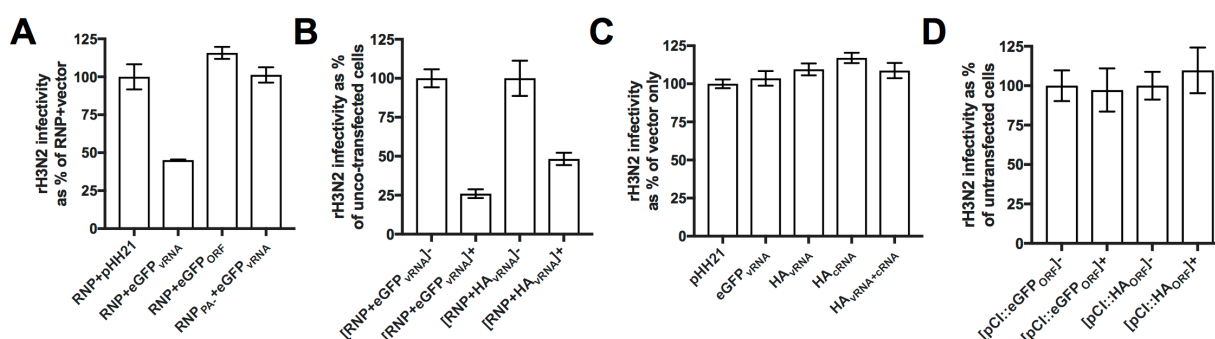241 nucleic acid products of viral genes processed by those complexes.
242

Figure 5. Activity of viral replication complexes is responsible for the inhibition on subsequent infection, not those viral gene products. (A) 293T cells were co-transfected with plasmids encoding the viral replicase complex proteins PB2, PB1, PA, and NP (RNP), together with 1 μg of either empty pHH21 vector, pHH21::eGFPvRNA (eGFP ORF flanked with NA UTRs), or pHH21::eGFPORF (eGFP ORF with no UTR sequence). Control cells were co-transfected with plasmids encoding the viral replicase complex minus PA, which was replaced by empty vector (RNPPA-), together with 1 μg of pHH21::eGFPvRNA. 24 hours post-transfection, cells were infected with rH3N2 at MOI=0.2 TCID50/cell. At 8 hpi, cells were harvested and assessed for rH3N2 infectivity via flow cytometry. rH3N2 infectivity are normalized to RNP+vector. **(B)** Similar experiment in (A) with co-transfection of RNP plasmids plus 1 μg of pHH21::eGFPvRNA or pHH21::HAvRNA. rH3N2 infectivity in co-transfected cells (eGFP+, HA+) are normalized to un-co-transfected cells (eGFP-, HA-) within the same culture wells. **(C)** Similar experiment in (A) with transfection of empty pHH21 vector, pHH21::eGFPvRNA, pHH21::HAvRNA, pHH21::HAcRNA, or pHH21::HAvRNA plus pHH21::HAcRNA. rH3N2 infectivity are normalized to empty pHH21 vector. **(D)** Similar experiment in (A) with transfection of pCI vector, pCI::eGFPORF or pCI::HAORF. rH3N2 infectivity in transfected cells (eGFP+, HA+) are normalized to un-transfected cells (eGFP-, HA-) within the same culture wells. Mean values (n=2 cell culture wells) ± standard deviations are shown.

243
244

Discussion

246 Superinfection plays an enormous role in influencing the outcome of IAV infection, both
247 by promoting reassortment and by facilitating the multiplicity reactivation of SIPs and
248 defective interferring particles (4). Despite this importance, the specific factors that govern
249 the occurrence of superinfection have remained obscure. Here, we reveal that IAV
250 superinfection susceptibility is directly regulated by the number of viral genes expressed
251 by a virion, regardless of their specific identity or function. This effect depends upon the
252 presence of active viral replication complexes, but not their nucleic acid or protein
253 products. Critically, we demonstrate that the presence of SIPs within viral populations
254 significantly increases the frequency of superinfection. This represents a completely novel
255 mechanism of viral superinfection exclusion and identifies a clear mechanistic
256 consequence of the enormous genomic heterogeneity within IAV populations.
257

258 The only other published study that examines IAV SIE in detail concluded that NA
259 expression mediates SIE by depleting the pool of available sialic acid receptors on the
260 cell surface(27). In this study, we directly quantified the contribution of NA expression to

8

261 SIE during IAV infection, and found that the SIE effect of NA expression is actually
262 comparable to that of other viral genes and that overall genomic content is the primary
263 determinant of superinfection potential. The conclusions of the Huang et al. study were
264 based primarily on two observations: (*1*) overexpression of NA within cells rendered them
265 refractory to infection by an HA-pseudotyped virus, and (*2*), IAV superinfection only
266 occured when cells were treated with NA inhibitors (NAIs)(27). While we cannot
267 conclusively explain the discrepancies between the two studies, we can offer a couple of
268 plausible explanations. First, the cellular overexpression studies in Huang et al. likely
269 involved levels of cellular NA expression that are far beyond those seen during IAV
270 infection. In fact, we were also able to observe a similarly potent restriction of IAV infection
271 following plasmid-driven NA overexpression (data not shown); however, this result did not
272 reflect what we observed during viral infection (**Fig 2**). Second, the observation that NAI
273 treatment dramatically increases superinfection frequencies may be explained by the
274 effects of cell death. In their experiments, Huang et al. infected cells at a relatively high
275 MOI, did not block secondary spread of the virus within cultures, and assessed
276 superinfection frequency at 20 hpi or later. Under these conditions, many of the initially
277 infected cells will be dead or dying and thus lost from the analysis. This may be especially
278 true of superinfected cells, which will tend to be infected at a higher than average effective
279 MOI. Even under low MOI conditions, we had to limit the timeframe of our experiments
280 and block secondary spread of virus to prevent cell death from skewing our results. NAI
281 treatment may act to help preserve co-infected cells so that they are detected at the
282 endpoint of the experiment, thus increasing the measured superinfection rate.

284 Our results reveal that SIE is mediated by multiple IAV genes in a dose-dependent fashion.
285 The surprising irrelevance of the specific IAV gene segments involved is explained by our
286 finding that the viral coding sequence of a gene segment can be replaced with that of
287 eGFP without any loss of inhibitory effect. This suggests a direct role for viral replicase
288 activity itself in triggering SIE, rather than any effect of the viral gene segments
289 themselves. The specific mechanism by which the activity of viral replicase complexes
290 may inhibit subsequent infection remains unclear, however one potential explanation is
291 that viral replication complexes trigger a dose-dependent intrinisic host anti-viral response.
292 While our experiments in Vero cells demonstrate that the secretion of type I IFN is not
293 required for SIE, they do not preclude the involvement of type I IFN-independent
294 mechanisms. These could include either the type III IFN-mediated induction of anti-viral
295 effectors, or the engagement of completely IFN-independent anti-viral mechanisms(41–
296 43). Future studies are aimed at delineating the role of the host in the regulation of IAV
297 superinfection.

299 Our results demonstrate that SIPs can directly influence the prevalence of superinfection,
300 and thus potentially the frequency of reassortment. Fonville et al. used a similar UV
301 irradiation-based method as shown here to demonstrate that increasing the frequency of
302 SIPs within a viral popuation increases the overall reassortment rate(40). The explanation
303 given for this effect was that increasing the abundance of SIPs increases the proportion
304 of the viral population that depends upon co-infection to replicate. As a result, within a
305 certain MOI range, a greater share of productively infected cells will be co-infected and
306 subject to reassortment. In our study, we confirmed this effect by observing a slight

307 increase in co-infection frequency with increasing UV dose when rPR8 and rH3N2 were
308 added simultaneously (**Fig 4E**). When we controlled for this however, we still observed a
309 significant increase in superinfection frequency as we increased the proportion of SIPs
310 through UV treatment (Fig 4D-F). Thus, the relationship between SIPs and SIE that we
311 describe here is completely independent of the increased multiplicity reactivation
312 observed by Fonville et al. and likely represents the effects of decreasing the strength of
313 SIE. Between these two studies, it is clear that SIPs can modulate the frequency of IAV
314 co-infection and reassortment though at least two distinct mechanisms.
315
316 IAV strains can differ significantly in the relative production and gene expression patterns
317 of SIPs(8,9). This raises the possibility that strains with distinct SIP production
318 phenotypes may differ in their reassortment potential, given the influence of SIPs over co-
319 infection and reassortment frequencies. If this is the case, it would suggest a significant
320 role for SIPs production in governing the evolutionary potential of IAV populations.
321
322 The relationship between viral gene expression patterns and superinfection exclusion that
323 we report here demonstrates that viral genomic heterogenity has distinct functional
324 consequences during infection. A crucial implication is that all infected cells cannot be
325 thought of as equal, but may in fact exhibit distinct phenotypes based on the number and
326 identity of viral genome segments they harbor. The relationship between viral genomic
327 heterogeneity and the phenotypic diversity of infected cells likely extends to other cellular
328 features beyond superinfection susceptibility.
329
330 It remains to be seen whether the relationship between viral gene dose and superinfection
331 susceptibility that we describe here exists for other segmented viruses besides IAV.
332 Beyond the segmented viruses, it has become increasingly clear that collective
333 interactions mediated by cellular co-infection significantly influence the replicative and
334 evolutionary dynamics of non-segmented viruses as well(44). More work is needed to
335 better understand the factors that govern co-infection for different virus families, both *in*
336 *vitro* and *in vivo*.
337
338 In summary, our work reveals a unique mechanism of IAV superinfection regulation that
339 is governed by viral genomic heterogeneity. Critically, we show that the abundance of
340 SIPs within a viral population directly influences the prevalence of superinfection;
341 suggesting that IAV strains may differ in their superinfection potential, and thus potential
342 for reassortment. This finding has significant consequences for understanding the
343 evolutionary potential of different IAV genotypes with varying SIP phenotypes. More
344 broadly, we demonstrate how genomic diversity within viral populations can have clear
345 functional consequences during infection.
346
347 **Methods**
348
349 **Plasmids**
350 The A/Puerto Rico/8/34 and A/Udorn/72 reverse genetics plasmids were generous gifts
351 from Dr. Adolfo Garcia-Sastre and Dr. Kanta Subbarao, respectively. The pCI vector wa
352 s graciously provided by Dr. Joanna Shisler. The pHH21::eGFP$_{vRNA}$ (eGFP ORF flanked

353   by the NA UTRs) was kindly gifted by Dr. Andrew Mehle. Generation of pHH21::HA$_{vRNA}$
354   has been previously described(9). The following primer pairs were used to generate the
355   indicated constructs. pHH21::eGFP$_{ORF}$ (BsmBI): 5' CGTCTCCTATTTTACTTGTACAGC
356   TCG; 3' CGTCTCCGGGATGGTGAGCAAGGGC. pHH21::HA$_{cRNA}$ (BsmBI): 5'CGTCTCA
357   TATTAGCAAAAGCAGG; 3' CGTCTCAGGGAGTAGAAACAAGGG. pCI::eGFP$_{ORF}$ (Eco
358   RI/SalI): 5' AGAATTCATGGTGAGCAAGG; 3'AGTCGACTTACTTGTACAGC. pCI::HA$_{OR}$
359   $_F$ (EcoRI/SalI): 5' AGAATTCATGGAAGATTTGTGCG; 3' AGTCGACCTAACTCAATGC
360   ATGTGT.

361

Cells

363   Madin-Darby canine kidney (MDCK) and human embryonic kidney HEK293T (293T) cells
364   were maintained in Gibco's minimal essential medium with GlutaMax (Life Technologies).
365   Vero cells were maintained in Dulbecco's modified eagle medium (Life Technologies).
366   Human lung epithelial A549 cells were maintained in Gibco's F-12 medium (Life
367   Technologies). MDCK, vero, and A549 cells were obtained from Dr. Jonathan Yewdell;
368   293T cells were obtained from Dr. Joanna Shisler. All media were supplemented with 8.3%
369   fetal bovine serum (Seradigm). Cells were grown at 37°C and 5% CO2.

370

Viruses

372   Recombinant A/Puerto Rico/8/1934 (rPR8) and rH3N2 viruses were generated using 8-
373   plasmid rescue systems. The rH3N2 virus is a reassortant with the HA and NA segments
374   from A/Udorn/72 (H3N2), the NS segment from A/California/04/09 (H1N1), and the other
375   5 segments from PR8. The rPR8 clones differ from the published sequence (GenBank
376   accession nos. AF389115–AF389122) at two positions: PB1 A549C (K175N) and HA
377   A651C (I207L) (numbering from initiating Met). Molecular clone-derived mutants (rPR8
378   NP:F346S and rPR8 NA:K239R) were generated using standard site-directed PCR
379   mutagenesis. All viruses were rescued by transfecting sub-confluent 293T cells with
380   500ng of each of the appropriate reverse genetics plasmids using JetPRIME (Polyplus)
381   according to the manufacturer's instructions. Plaque isolates derived from rescue
382   supernatants were amplified into seed stocks in MDCK cells. Working stocks were
383   generated by infecting MDCK cells at an MOI of 0.0001 TCID50/cell with seed stock and
384   collecting and clarifying supernatants at 48 hpi. All viral growth was carried out in MEM
385   with 1 µg/mL trypsin treated with L-(tosylamido-2-phenyl) ethyl chloromethyl ketone
386   (TPCK-treated trypsin; Worthington), 1mM HEPES, and 100 µg/mL gentamicin. Virus
387   stocks were titered via standard tissue culture infectious dose 50 (TCID50) assay.

388

Superinfection assay

390   For the 6hr sequential infection group, confluent mammalian cells (MDCK, vero, A549, or
391   293T) in six-well plates were infected with rPR8 at MOI<0.3 TCID50/cell for 1 hour. 1 hour
392   post-adsorption, monolayers were washed with PBS and incubated in serum-containing
393   medium. At 3 hpi, neutralizing anti-PR8-HA mouse mAb H17-L2 (5 µg/mL) was added to
394   cultures to prevent spread of rPR8. At 6 hpi, monolayers were superinfected with rH3N2
395   at MOI<0.3 TCID50/cell in the presence of H17-L2 (which does not interfere with rH3N2
396   infection, Fig S2). 1 hour post-adsorption, monolayers were washed with PBS and
397   incubated in serum-containing medium with H17-L2. At 9 hpi of rPR8 (3 hpi of rH3N2),
398   the media was changed to MEM with 50 mM Hepes and 20 mM NH4Cl to block spread

11

399 of both viruses. At 19 hpi of rPR8 (13 hpi of rH3N2), monolayers were trypsinized into
400 single-cell suspensions.
401
402 For the 0hr simultaneous infection group, cells were infected with a mixture of rPR8 and
403 rH3N2 at the same MOIs as in 6hr superinfection group. At 3 hpi, the NH4Cl media was
404 added to block viral spread and cells were harvested at 19 hpi.
405
406 All cells were simultaneously fixed and permeabilized using foxP3 fix/perm buffer
407 (eBioscience). Fixed cells were stained with Alexa Fluor 488-conjugated mouse anti-H1
408 mAb H36-26 (which does not compete with H17-L2), Pacific Orange-conjugated mouse
409 anti-N1 mAb NA2-1C1, Pacific Blue-conjugated mouse anti-NS1 mAb NS1-1A7 and
410 Alexa Fluor 647-conjugated mouse anti-H3 mAb H14-A2 (All mAbs gifts of Dr. Jon
411 Yewdell). After staining, cells were washed, run on a BD LSR II, and analyzed using
412 FlowJo version 10.1 (Tree Star, Inc.).
413
414 **Quantification of NA expression**
415 H1+N1+ MDCK cells infected with rPR8WT, rPR8 NP:F346S, or rPR8 NA:K239R in the
416 superinfection assay (6hr group) were gated and histograms for NA expression were
417 plotted. The geometric mean fluorescence intensities (GMFI) for NA were determined
418 using FlowJo version 10.1 (Tree Star, Inc.).
419
420 **UV treatment and analysis**
421 rPR8 stocks were placed in six-well plates on ice (500 ul/well). Plates were placed 5 cm
422 underneath a 302nm UVP-57 handheld UV lamp (UVP) and irradiated for 30s or 60s.
423 TCID50 titers and single virion expression patterns of untreated and UV-treated virus
424 were determined on MDCK cells, and superinfection assays described above were
425 performed using these viruses and rH3N2.
426
427 **Transfection assay**
428 80% confluent 293T cells in six-well plates were transfected with the following plasmids
429 using jetPRIME (Polyplus): RNP (500 ng each of pDZ::PB2, pDZ::PB1, pDZ::PA, and
430 pDZ::NP) plus 1 μg of pHH21 vector; RNP plus 1 μg of pHH21::eGFP$_{vRNA}$ (eGFP$_{ORF}$
431 flanked with NA UTRs); RNP plus 1 μg of pHH21::eGFP$_{ORF}$; RNP plus 1 μg of
432 pHH21::HA$_{vRNA}$; RNP$_{PA-}$ (500 ng each of pDZ::PB2, pDZ::PB1, pDZ, and pDZ::NP) plus 1
433 μg of pHH21::eGFP$_{vRNA}$; RNP$_{PA-}$ plus 1 μg of pHH21::HA$_{vRNA}$; 6 μg of pHH21 vector; 3 μg
434 of pHH21 vector plus 3 μg of pHH21::eGFP$_{vRNA}$; 3 μg of pHH21 vector plus 3 μg of
435 pHH21::HA$_{vRNA}$; 3 μg of pHH21 vector plus 3 μg of pHH21::HA$_{cRNA}$; 3 μg of
436 pHH21::HA$_{vRNA}$ plus 3 μg of pHH21::HA$_{cRNA}$; 3 μg of the pCI vector; 3 μg of pCI::eGFP$_{ORF}$;
437 3 μg of pCI::HA$_{ORF}$. All plasmid-encoded viral sequences were derived from PR8. 24
438 hours post transfection, monolayers were infected with rH3N2 at an MOI of 0.2
439 TCID50/cell. At 8 hpi, cells transfected by RNP+pHH21 and pCI plasmids were harvested
440 and stained with Alexa Fluor 488-conjugated mouse anti-H1 mAb H36-26 and Alexa Fluor
441 647-conjugated mouse anti-M2 mAb O19. Cells transfected with pHH21 plasmids were
442 permeabilized, fixed and stained with Alexa Fluor 647-conjugated mouse anti-NP mAb
443 HB-65. After staining, cells were washed, run on a BD LSR II, and virus infection
444 frequencies, as measured by fractions of M2+ or NP+ cells, were quantified using FlowJo

445 version 10.1 (Tree Star, Inc.).
446
447 **Statistical analysis**
448 Unpaired, two-sided student's t-tests were applied to the data shown in Fig 1B, Fig 2B,
449 Fig 3A, Fig 3B, and Fig 4F. An unpaired, two-sided Welch's t-test was applied to the data
450 shown in Fig 3D. All statistical analyses were performed with GraphPad Prism 7.0a.
451

458 **References**
459
460 1. Iuliano AD, Roguski KM, Chang HH, Muscatello DJ, Palekar R, Tempia S, et al.
461   Estimates of global seasonal influenza-associated respiratory mortality: a modelling
462   study. The Lancet [Internet]. 2017 Dec [cited 2017 Dec 14]; Available from:
463   http://linkinghub.elsevier.com/retrieve/pii/S0140673617332932

464 2. Taubenberger JK, Morens DM. Influenza: the once and future pandemic. Public
465   Health Rep Wash DC 1974. 2010 Apr;125 Suppl 3:16–26.

466 3. Brooke CB. Biological activities of "noninfectious" influenza A virus particles. Future
467   Virol. 2014 Jan;9(1):41–51.

468 4. Brooke CB. Population Diversity and Collective Interactions during Influenza Virus
469   Infection. J Virol. 2017 Nov 15;91(22).

470 5. McDonald SM, Nelson MI, Turner PE, Patton JT. Reassortment in segmented RNA
471   viruses: mechanisms and outcomes. Nat Rev Microbiol. 2016 Jul;14(7):448–60.

472 6. Lowen AC. Constraints, Drivers, and Implications of Influenza A Virus
473   Reassortment. Annu Rev Virol [Internet]. 2017 Sep 29 [cited 2017 Jun 8];4(1).
474   Available from: http://www.annualreviews.org/doi/10.1146/annurev-virology-
475   101416-041726

476 7. Taubenberger JK, Kash JC. Influenza virus evolution, host adaptation, and
477   pandemic formation. Cell Host Microbe. 2010 Jun 25;7(6):440–51.

478 8. Brooke CB, Ince WL, Wrammert J, Ahmed R, Wilson PC, Bennink JR, et al. Most
479   influenza a virions fail to express at least one essential viral protein. J Virol. 2013
480   Mar;87(6):3155–62.

481 9. Brooke CB, Ince WL, Wei J, Bennink JR, Yewdell JW. Influenza A virus
482   nucleoprotein selectively decreases neuraminidase gene-segment packaging while
483   enhancing viral fitness and transmissibility. Proc Natl Acad Sci U S A. 2014 Nov
484   25;111(47):16854–9.

485   10. Hirst GK. Mechanism of influenza recombination. Virology. 1973 Sep;55(1):81–93.

486   11. Hirst GK, Pons MW. Mechanism of influenza recombination. Virology. 1973
487   Dec;56(2):620–31.

488   12. Russell AB, Trapnell C, Bloom JD. Extreme heterogeneity of influenza virus
489   infection in single cells. eLife [Internet]. 2018 Feb 16 [cited 2018 Mar 15];7.
490   Available from: https://elifesciences.org/articles/32303

491   13. Dou D, Hernández-Neuta I, Wang H, Östbye H, Qian X, Thiele S, et al. Analysis of
492   IAV Replication and Co-infection Dynamics by a Versatile RNA Viral Genome
493   Labeling Method. Cell Rep. 2017 Jul;20(1):251–63.

494   14. White DO, Cheyne IM. Early events in the eclipse phase of influenza and
495   parainfluenza virus infection. Virology. 1966 May;29(1):49–59.

496   15. White DO, Day HM, Batchelder EJ, Cheyne IM, Wansbrough AJ. DELAY IN THE
497   MULTIPLICATION OF INFLUENZA VIRUS. Virology. 1965 Feb;25:289–302.

498   16. Ramig RF. Superinfecting rotaviruses are not excluded from genetic interactions
499   during asynchronous mixed infections in vitro. Virology. 1990 May;176(1):308–10.

500   17. Keirstead ND, Coombs KM. Absence of superinfection exclusion during
501   asynchronous reovirus infections of mouse, monkey, and human cell lines. Virus
502   Res. 1998 Apr;54(2):225–35.

503   18. Nethe M, Berkhout B, van der Kuyl AC. Retroviral superinfection resistance.
504   Retrovirology. 2005 Aug 18;2:52.

505   19. Schaller T, Appel N, Koutsoudakis G, Kallis S, Lohmann V, Pietschmann T, et al.
506   Analysis of hepatitis C virus superinfection exclusion by using novel fluorochrome
507   gene-tagged viral genomes. J Virol. 2007 May;81(9):4591–603.

508   20. Tscherne DM, Evans MJ, von Hahn T, Jones CT, Stamataki Z, McKeating JA, et al.
509   Superinfection exclusion in cells infected with hepatitis C virus. J Virol. 2007
510   Apr;81(8):3693–703.

511   21. Zou G, Zhang B, Lim P-Y, Yuan Z, Bernard KA, Shi P-Y. Exclusion of West Nile
512   virus superinfection through RNA replication. J Virol. 2009 Nov;83(22):11765–76.

513   22. Zhang X-F, Sun R, Guo Q, Zhang S, Meulia T, Halfmann R, et al. A self-
514   perpetuating repressive state of a viral replication protein blocks superinfection by
515   the same virus. Wang A, editor. PLOS Pathog. 2017 Mar 7;13(3):e1006253.

516   23. Laliberte JP, Moss B. A novel mode of poxvirus superinfection exclusion that
517   prevents fusion of the lipid bilayers of viral and cellular membranes. J Virol. 2014
518   Sep 1;88(17):9751–68.

519 24. Folimonova SY. Superinfection exclusion is an active virus-controlled function that
520   requires a specific viral protein. J Virol. 2012 May;86(10):5554–61.

521 25. Simon KO, Cardamone JJ, Whitaker-Dowling PA, Youngner JS, Widnell CC.
522   Cellular mechanisms in the superinfection exclusion of vesicular stomatitis virus.
523   Virology. 1990 Jul;177(1):375–9.

524 26. Ludlow M. Measles virus superinfection immunity and receptor redistribution in
525   persistently infected NT2 cells. J Gen Virol. 2005 Aug 1;86(8):2291–303.

526 27. Huang I-C, Li W, Sui J, Marasco W, Choe H, Farzan M. Influenza A virus
527   neuraminidase limits viral superinfection. J Virol. 2008 May;82(10):4834–43.

528 28. Holmes EC, Ghedin E, Miller N, Taylor J, Bao Y, St George K, et al. Whole-
529   Genome Analysis of Human Influenza A Virus Reveals Multiple Persistent
530   Lineages and Reassortment among Recent H3N2 Viruses. Levin S, editor. PLoS
531   Biol. 2005 Jul 26;3(9):e300.

532 29. Rambaut A, Pybus OG, Nelson MI, Viboud C, Taubenberger JK, Holmes EC. The
533   genomic and epidemiological dynamics of human influenza A virus. Nature. 2008
534   May 29;453(7195):615–9.

535 30. Nelson MI, Edelman L, Spiro DJ, Boyne AR, Bera J, Halpin R, et al. Molecular
536   Epidemiology of A/H3N2 and A/H1N1 Influenza Virus during a Single Epidemic
537   Season in the United States. Kawaoka Y, editor. PLoS Pathog. 2008 Aug
538   22;4(8):e1000133.

539 31. Nelson MI, Viboud C, Simonsen L, Bennett RT, Griesemer SB, St. George K, et al.
540   Multiple Reassortment Events in the Evolutionary History of H1N1 Influenza A
541   Virus Since 1918. Kawaoka Y, editor. PLoS Pathog. 2008 Feb 29;4(2):e1000012.

542 32. Westgeest KB, Russell CA, Lin X, Spronken MIJ, Bestebroer TM, Bahl J, et al.
543   Genomewide analysis of reassortment and evolution of human influenza A(H3N2)
544   viruses circulating between 1968 and 2011. J Virol. 2014 Mar;88(5):2844–57.

545 33. Maljkovic Berry I, Melendrez MC, Li T, Hawksworth AW, Brice GT, Blair PJ, et al.
546   Frequency of influenza H3N2 intra-subtype reassortment: attributes and
547   implications of reassortant spread. BMC Biol. 2016 Dec 29;14(1):117.

548 34. Marshall N, Priyamvada L, Ende Z, Steel J, Lowen AC. Influenza Virus
549   Reassortment Occurs with High Frequency in the Absence of Segment Mismatch.
550   Basler CF, editor. PLoS Pathog. 2013 Jun 13;9(6):e1003421.

551 35. Fukuyama S, Katsura H, Zhao D, Ozawa M, Ando T, Shoemaker JE, et al. Multi-
552   spectral fluorescent reporter influenza viruses (Color-flu) as powerful tools for in
553   vivo studies. Nat Commun. 2015 Mar 25;6:6600.

36. Desmyter J, Melnick JL, Rawls WE. Defectiveness of interferon production and of rubella virus interference in a line of African green monkey kidney cells (Vero). J Virol. 1968 Oct;2(10):955–61.

37. Emeny JM, Morgan MJ. Regulation of the interferon system: evidence that Vero cells have a genetic defect in interferon production. J Gen Virol. 1979 Apr;43(1):247–52.

38. Gulati S, Lasanajak Y, Smith DF, Cummings RD, Air GM. Glycan array analysis of influenza H1N1 binding and release. Marino PA, editor. Cancer Biomark. 2014 Feb 27;14(1):43–53.

39. Hensley SE, Das SR, Gibbs JS, Bailey AL, Schmidt LM, Bennink JR, et al. Influenza A virus hemagglutinin antibody escape promotes neuraminidase antigenic variation and drug resistance. PloS One. 2011;6(2):e15190.

40. Fonville JM, Marshall N, Tao H, Steel J, Lowen AC. Influenza Virus Reassortment Is Enhanced by Semi-infectious Particles but Can Be Suppressed by Defective Interfering Particles. PLoS Pathog. 2015 Oct;11(10):e1005204.

41. Dixit E, Boulant S, Zhang Y, Lee ASY, Odendall C, Shum B, et al. Peroxisomes Are Signaling Platforms for Antiviral Innate Immunity. Cell. 2010 May;141(4):668–81.

42. Wack A, Terczyńska-Dyla E, Hartmann R. Guarding the frontiers: the biology of type III interferons. Nat Immunol. 2015 Jul 21;16(8):802–9.

43. Odendall C, Kagan JC. The unique regulation and functions of type III interferons in antiviral immunity. Curr Opin Virol. 2015 Jun;12:47–52.

44. Sanjuán R. Collective Infectious Units in Viruses. Trends Microbiol. 2017 May;25(5):402–12.

Figure Legends

Figure 1. A 6-hr delay between primary infection and superinfection allows robust superinfection exclusion. The indicated mammalian cell lines were either simultaneously (0hr) or sequentially (6hr) infected with rPR8 and rH3N2 at MOI<0.3 TCID50/cell. **(A)** Representative FACS plots showing expression of H1 versus H3 within MDCK cells. **(B)** H3+ frequencies within H1+ cells following simultaneous or sequential infection, in the indicated cell lines. Values are calculated as the percentage of the mean 0hr value, and are presented as the mean (n=3 cell culture wells) ± standard deviations. ***$P<0.001$; ****$P<0.0001$; t test.

Figure 2. Superinfection is more potently inhibited in NA positive cells, independent of NA expression level. MDCK cells were infected with rPR8$_{WT}$, rPR8$_{NP:F346S}$ or rPR8$_{NA:K239R}$, and simultaneously (0hr) or sequentially (6hr) infected with

593 rH3N2; all infections at MOI<0.3 TCID50/cell. **(A)** Representative FACS plots comparing
594 H3+ frequencies between H1+N1- and H1+N1+ cells. **(B)** H3+ frequencies within H1+N1-
595 and H1+N1+ cells following simultaneous (0hr) or sequential (6hr) infection. Values are
596 calculated as the percentage of the mean 0hr value. **(C)** Comparison of NA expression
597 within H1+N1+ cells between rPR8$_{WT}$, rPR8$_{NP:F346S}$ and PR8$_{NA:K239R}$ at 19 hpi. **(D)**
598 Comparison of H3+ frequencies within H1+N1- and H1+N1+ cells following sequential
599 infection (6hr) between the three indicated viruses. Values are normalized to H3+
600 frequencies in simultaneous infection (0hr) controls. For data in Fig B and D, mean values
601 (n=3 cell culture wells) ± standard deviations are shown. **P<0.01; ****P<0.0001; *t* test.
602
603 **Figure 3. Superinfection is more frequent in cells that express fewer viral genes.**
604 MDCK cells were infected with rPR8, and simultaneously (0hr) or sequentially (6hr)
605 infected with rH3N2; all infections at MOI<0.3 TCID50/cell. **(A)** H3+ frequencies within
606 N1+H1- and N1+H1+ cells following simultaneous (0hr) or sequential (6hr) infection.
607 Values are calculated as the percentage of the mean 0hr value. **(B)** H3+ frequencies
608 within H1+NS1- and H1+NS1+ cells following simultaneous (0hr) or sequential (6hr)
609 infection. Values are calculated as the percentage of the mean 0hr value. **(C)** Comparison
610 of H3+ percentages between 8 cell populations gated based on the expression of the
611 indicated combinations of 3 PR8 gene products (HA, NA, NS1). Data represents the
612 values obtained from 6hr samples normalized to the values obtained from 0hr control
613 samples. Each data point represents the value for the indicated cell population within a
614 single cell culture well. **(D)** Data in C grouped by total numbers of expressed viral gene
615 products rather than their specific identity. **P<0.01; ***P<0.001; *t* test.
616
617 **Figure 4. Superinfection is more common in viral populations that contain more**
618 **SIPs.** rPR8 was irradiated with 302nm UV lamp for 30s or 60s. **(A)** TCID50 titers of
619 untreated (0s), 30s, and 60s UV-treated rPR8. Data from two independent experiments
620 are shown. **(B)** Representative FACS plots showing HA and NA expression patterns of
621 untreated (0s) and 60s UV-treated rPR8. **(C)** Quantification of HA/NA co-expression in
622 infected cells from (B). **(D-F)** MDCK cells were infected with untreated (0s), 30s, or 60s
623 UV-treated rPR8 at an MOI of 0.04 NAEU/cell, and simultaneously (0hr) or sequentially
624 (6hr) infected with rH3N2 at MOI<0.3 TCID50/cell. **(D)** Representative FACS plots
625 showing expression of N1 versus H3 in cells infected with either untreated (0s) or 60s
626 UV-treated rPR8. **(E)** rH3N2 infection percentages within N1+ cells infected with either
627 untreated (0s), 30s, or 60s UV-treated rPR8. **(F)** Data from 6hr samples in E shown as %
628 of 0hr control samples. For Fig C, E, and F, mean values (n=3 cell culture wells) ±
629 standard deviations are shown. **P<0.01; *t* test.
630
631 **Figure 5. Activity of viral replication complexes is responsible for the inhibition on**
632 **subsequent infection, not those viral gene products. (A)** 293T cells were co-
633 transfected with plasmids encoding the viral replicase complex proteins PB2, PB1, PA,
634 and NP (RNP), together with 1 μg of either empty pHH21 vector, pHH21::eGFP$_{vRNA}$
635 (eGFP ORF flanked with NA UTRs), or pHH21::eGFP$_{ORF}$ (eGFP ORF with no UTR
636 sequence). Control cells were co-transfected with plasmids encoding the viral replicase
637 complex minus PA, which was replaced by empty vector (RNP$_{PA-}$), together with 1 μg of
638 pHH21::eGFP$_{vRNA}$. 24 hours post-transfection, cells were infected with rH3N2 at MOI=0.2

TCID50/cell. At 8 hpi, cells were harvested and assessed for rH3N2 infectivity via flow cytometry. rH3N2 infectivity are normalized to RNP+vector. **(B)** Similar experiment in (A) with co-transfection of RNP plasmids plus 1 μg of pHH21::eGFP$_{vRNA}$ or pHH21::HA$_{vRNA}$. rH3N2 infectivity in co-transfected cells (eGFP+, HA+) are normalized to un-co-transfected cells (eGFP-, HA-) within the same culture wells. **(C)** Similar experiment in (A) with transfection of empty pHH21 vector, pHH21::eGFP$_{vRNA}$, pHH21::HA$_{vRNA}$, pHH21::HA$_{cRNA}$, or pHH21::HA$_{vRNA}$ plus pHH21::HA$_{cRNA}$. rH3N2 infectivity are normalized to empty pHH21 vector. **(D)** Similar experiment in (A) with transfection of pCI vector, pCI::eGFP$_{ORF}$ or pCI::HA$_{ORF}$. rH3N2 infectivity in transfected cells (eGFP+, HA+) are normalized to un-transfected cells (eGFP-, HA-) within the same culture wells. Mean values (n=2 cell culture wells) ± standard deviations are shown.

Supporting information

Figure S1. Expression of HA, NA, and NS1 by rPR8 and rH3N2 can be differentiated using specific mAbs. MDCK cells were infected with rPR8 or rH3N2 at an MOI<0.3 TCID50/cell. At 19 hpi, cells were harvested, fixed, permeabilized, stained against H1 (H36-26), N1 (NA2-1C1), NS1 (1A7), and H3 (H14-A2), and run on an LSR II flow cytometer. Expression of H1 versus N1, and NS1 versus H3 are shown in representative FACS plots.

Figure S2. Superinfection is inhibited in multiple cell lines. H1 versus H3 expression in Vero cells, A549 cells, and 293T cells observed in the experiments described in Fig 1 are shown in as representative FACS plots.

Figure S3. Gating scheme for measuring superinfection frequencies in cells that express different rPR8 genes. Cells from the experiment described in Fig 3C,D were assessed for expression of HA, NA and NS sequentially. The fractions of H3+ cells (indicative of superinfection rates) were quantified and compared between each of the eight cell populations with the indicated expression patterns.

Figure S4. Cells co-transfected with plasmids encoding viral replicase and viral vRNA are less susceptible to subsequent infection. Cells from the experiments described in Fig 5A,B are assessed for expression of M2 (indicative of rH3N2 infection) versus eGFP and HA (indicative of co-transfection) in representative FACS plots.

Figure S5. Overexpression of mRNA and protein does not inhibit subsequent infection. (A) Cells from the experiment described in Fig 5D are assessed for expression of M2 (indicative of rH3N2 infection) versus eGFP and HA (indicative of transfection) in representative FACS plots. **(B)** rH3N2 infectivity in A are shown as % of pCI vector. Mean values (n=2 cell culture wells) ± standard deviations are shown.